Doping, Vacancy formation and Substitutional Effects on Semiconductor Selectivity of Rutile TiO 2 Crystal

Article · February 2013

CITATIONS
0

READS
227

2 authors:

Aqeel Mohsin Ali
University of Basrah
16 PUBLICATIONS **12** CITATIONS
SEE PROFILE

Ali Almowali
University of Basrah
48 PUBLICATIONS **87** CITATIONS
SEE PROFILE

Chemistry and Materials Research
ISSN 2224- 3224 (Print) ISSN 2225- 0956 (Online)
Vol.3 No.2, 2013

Doping, Vacancy formation and Substitutional Effects on Semiconductor Selectivity of Rutile TiO_2 Crystal

Aqeel M. Ali[1] Ali H. Al-Mowali[2*]

1. Department of Physics, College of Science, University of Basrah, Basrah, Iraq
2. Department of Chemistry, College of Science, University of Basrah, Basrah, Iraq

* E-mail of the corresponding author: ali_almoali@yahoo.com

Abstract

We have investigated the energy band structure and electronic transitional spectra of rutile and oxygen point defect/substitution of X-rutile (X= B, C and N atoms) by using the Hartree-Fock and density functional theories calculations based on STO-3G basis set. Our calculated results showed that the oxygen vacancy enhanced the photocatalytic activity at the visible light range, due to mid gap induced states. In substitutional X to O doped rutile, the transition of excited electrons may induce a red shift of optical absorption edge, that may result due to donor state produced by doping atoms. Our results also indicated that the theoretical investigation can provide important information and good prediction of semiconductor properties.

Keywords: Ceramic, Rutile, Vacancy, Doped TiO_2, ab initio, DFT

1. Introduction

Strong oxidation and reduction power of photoexcited titanium dioxide (TiO_2) was realized from the discovery of the Honda-Fujishima effect (Fujishima & Honda 1972). Photocatalytic reactions at the surface of titanium dioxide have attracted much attention in view of their practical applications to environmental cleaning such as self cleaning of tiles, glasses and windows. Additionally, it can be used as an antibacterial agent (Nakata & Fujishima 2012) because of its strong oxidation activity and super hydrophilicity. TiO_2 showed a relatively high reactivity (Liu *et al.* 2009) under ultraviolet light (λ <387nm), whose energy exceeds the band gap of 3.3 eV in the anatase crystalline phase (Ali 2012). The development of photocatalysts exhibiting high reactivity under visible light (λ > 400 nm) should allow the main part of the solar spectrum, even under poor illumination of interior lighting, to be used. Several approaches for TiO_2 modification have been proposed: metal-ion implanted TiO_2 (Wang *et al.* 2007), reduced TiOx photocatalysts (Cho & Han 2006), non-metal doped-TiO_2 (Lee *et al.* 2012), composites of TiO_2 with semiconductor having lower band gap energy, sensitizing of TiO_2 with dyes and TiO_2 doped with upconversion luminescence agent.

Oxygen vacancies are considered to be important reactive agents for many adsorbates (Zhang *et al.* 2010) and hence, many surface reactions are influenced by these point defects (Grigorov *et al.* 2011). Incorporation of boron into TiO_2 (In *et al.* 2007) could extend the spectral response to the visible region (Jinlong *et al.* 2010) and the photocatalytic activity is greatly enhanced as it is further loaded (Janus *et al.* 2009). A carbon-doped nanostructured TiO_2 material will have an optical band gap lower than 2.1 eV (Park *et al.* 2009). The visible-light photocatalytic activity of nitrogen-doped TiO_2 materials was reported (Wang *et al.* 2010). Doping (Mitoraj & Kisch 2008) seems to induce the band-gap narrowing at high N-loadings (Gorska *et al.* 2009).

Here, we considered the rutile polymorph and studied the electronic properties and electronic spectrum of substitutional X-doped (where X= B, C and N atoms) rutile TiO_2 systematically using Hartree-Fock and density functional theories calculations.

2. Computational Methodology

We employed several methods: Hartree-Fock theory (HF) and Density Functional Theory (DFT). The pure DFT combines exact Hartree-Fock electron exchange functional with different types of posterior electron correlation corrections to the total energy such as local and non-local correlation of Lee-Yang-Parr (HFLYP), Perdew-Zunger81 (HFPZ81) and local spin density correlation of Vosko-Wilk-Nusair (HFVWN). Calculations were carried out with an all-electron Slater Type Orbitals basis set (STO-3G). The computations were performed using the Hyperchem-7.52 computer package (Hyperchem 7.52 2005). The electronic spectral (electron transition states)

search was carried out using configuration interaction CI under the semiempirical PM3 method, within the excitation energy about 5 eV. Our crystal parameters of unit bulk rutile were taken from the reference (Shirley *et al.* 2010) Figure 1. The first one is that an oxygen atom in the crystal unit will make a vacancy, and then will be replaced by X atom like (B, C and N atoms) as shown in Table 1. All calculations were done without any re-optimization, because the very small changes that took place under substitutional operations were proven by theoretical (Pan *et al*. 2010) and experimental studies (Di Valentin *et al.* 2007).

3. Results And Discussion

While HF and DFT are known to underestimate band gap up to 50%, it is possible to make qualitative statements regarding the influence of dopants. Rutile is a semiconductor with a band gap E_g of 3.03 eV. In the present study, the band structure was computed for pure rutile, oxygen vacancy point defect and as a function of atomic number of dopant atoms.

3.1 Electronic structure

The calculated direct band gap E_g values, obtained with HF, HFVWN, HFPZ81 and HFLYP as a function of atomic number of dopants, are showed in Figure 2. The direct band gap showed a non-linearly behavior with decreasing the atomic number of substitutional dopant atoms. The larger value is identified by carbon, while the narrower values are achieved by the substitutional atoms of boron B. Nitrogen dopant reduced the band gap of rutile TiO_2 with small variation in magnitudes, in particular, a very small reduction in the fundamental band gap of TiO_2 with few contents of nitrogen atom has been verified by experiments (Cao *et al.* 2009). We have calculated the highest filled/half-filled states and the lowest unfilled states for all doping-TiO_2. These two energy states of pure and doped rutile are shown in Figure 3. The two dotted lines are placed to make the mid gap states easy to be distinguished. The corresponding Fermi energy levels were estimated by equation (Di Valentin *et al.* 2007):

$$E_F = E - 0.5\, E_g \qquad (1)$$

where E is the energy related to the bottom of the conduction band. Figure 4 showed how Fermi energy level varies with the atomic number of dopants. Oxygen and dopants are not all isovalent, thus, dopants substitution for oxygen in rutile TiO_2 changed the electronic structure. Also, dopants may make sub-bands of donor states within the midgap of the material and, therefore, the Fermi level will shift away from its ideal mid gap position. From the analysis of Figure 4, the upper limit is associated with atomic number of (B=5, C=6), and all modified rutiles are n-type semiconductors. Figure-5 displays the theoretical absorption behavior of pure rutile. TiO_2 exhibited high transmittance in the visible region with a sharp absorption edge between 350 and 400 nm, which is recently approved experimentally (Landmann *et al.* 2012). The optical band gap for direct allowed transition is about 3.0 eV, as it can be calculated from Figure 5, which is in good agreement with the experimental value of rutile.

3.2 Vacancy And Point Defects

3.2.1. Oxygen vacancy defect

It is classified as a fundamental native point defect. Typically, by theoretical expectations native defects in wide gap semiconductors do introduce deep levels inside the band gap. Table 2, shows the calculated electronic states of defected TiO_2 beside pure TiO_2. The most important feature of Table 2 is that the point defect of oxygen vacancy introduces a defect level inside the TiO_2 fundamental band gap state. The extended band state of oxygen vacancy is a donor and the conduction band edge states have the titanium *3d* character, while the valence band edge states have the oxygen *2p* character. The oxygen vacancy is a double donor because the O-atom has two additional electrons transferred from the three surrounding Ti-atoms, thus, when the O-atom is removed as a neutral atom (breaking the Coulomb bindings with three neighboring Ti to free an O) the two extra electrons make the vacancy a double donor. This defect-induced electronic state is a delocalized resonant, and according to this the vacancy is not a charge carrier trap. The Fermi energy level is moved into the conduction band, so there is a significant filling of the defect state. Experimental studies measured that neutral oxygen vacancy point defect produced peaks 1.18 and 1.2 eV below the bottom of the pure TiO_2 conduction band. Theoretical investigation by using numerical discrete variation and semiempirical methods, observed defect peaks 0.87 and 0.7 eV, respectively, below conduction band for neutral defect. Another theoretical study based on density functional theory with two levels, local density approximation LDA and generalized gradient approximation GGA, showed that the mid gap states are located at 0.1 and 0.3 eV below the conduction band.

In the present study, the calculated values for vacancy defect state indicate a doubly occupied midgap level below

the bottom of the conduction band edge displayed in Table 3. These differences agree with other theoretical studies which show that differences are considerably smaller than the experimental values. Thus, our investigation predicts that oxygen vacancy produces a filled mid gap state, with small shifting below conduction band edge. The formation of oxygen vacancy, creates a filled Ti *3d* band at the Fermi level and hence, the possibility of Stoner splitting of the *3d* band.

The theoretical electronic spectra of oxygen deficient rutile in Figure 6, show a blue shifting in UV absorption towards shorter wavelength 300 nm. The important electronic transition is induced at the visible range with three peaks which were produced by oxygen point defect. The stronger absorption took place at long wavelength λ=672 nm. Two peaks appeared at 550 nm and 430 nm which had low oscillator strengths. According to this, oxygen vacancy plays an important role to enhance TiO_2 photocatalytic activity in the visible region.

3.2.2 Boron substitution (B_s)

Recently, boron-modified TiO_2, under UV-visible light, has been successfully prepared and exhibited high photocatalytic activity. In the present study, One O-atom was substituted by a B-atom. In this model, the lattice remains neutral but an unpaired electron is introduced. The unpaired electron was introduced due to the formal substitution of O^{-2} by B^{+} (replacing O-atom with high electronegativity 3.44 by B-atom with moderate electronegativity 2.04) which was localized on one of Ti-atoms nearest B^{+}. Thus, one titanium which was formally Ti^{+4} became Ti^{+3}. The electronic properties of the singly B-doped rutile were investigated. Boron defect produced a half filled electronic state with the same energy of the bottom conduction band beside an unfilled state inside the fundamental conduction band of rutile, and these results are displayed Table 4. This minority spin state is composed of titanium 3d orbitals, which were accompanied with band gap reducing with about 0.5-0.8 eV for doped lattice. There are contrary reports on the effect of boron modification on the band gap, and a red shift in the band gap of titanium was seen.

Theoretical UV-visible spectra for boron-doped rutile are depicted in Figure 7. Evidently, a red shift can be observed in the direct band gap of B-substituted rutile when compared to the undoped TiO_2 and is confirmed from the oscillator strength versus wavelength plot shown as inset in Figure 7. Authors testified that boron doping led to the response to visible light. The UV-Visible spectra indication showed greater absorption in the visible region for boron-doped titanium. Maximum activity occurred at a low concentration of boron probably presented substitutionally at oxygen sites, which has been reported.

3.2.3 Carbon substitution (C_s)

TiO_2 doped with a nonmetal impurity can provide effective modification of the electronic structure and higher activity under visible light. In the literatures, the carbon dopant has been described as a negative ion that replaces oxygen substitution in the lattice. Our calculations of C-doped rutile proved that C-defect produces a filled electron state by 0.5 eV below the fundamental conduction band. The calculated valence and conduction band edges and the carbon-substitution point defect states, by HF and DFT methods were summarized in Table 5. C-doped rutile gave rise to localized C *2p* donor states, and induced visible light photoactivity, which was proved by other researchers. The incorporation of carbon into the rutile lattice influenced the band edges of the former energy gap drifts by 0.03-0.07 eV, depending on the correlation function. Another feature presented in this work, is the high shifting away of the Fermi energy level E_F towards the essential conduction band. E_F is shifted by more than 1.5 eV. Our theoretical studies about carbon-doped TiO_2 clarified the origin of the red shift of optical absorption edge of the doped TiO_2, which exhibited significant absorption in the visible region, as shown in Figure 8. The C-doped rutile exhibited significant absorption in the visible region, in addition to the absorption band at wavelength below 400 nm. Experimentally, a carbon-doped nanostructured TiO_2 material having an optical band gap lower than 2.1 eV, could be utilized as a photocatalyst in solar energy conversion devices and gas sensors.

3.2.4 Nitrogen substitution (N_s)

Doping of TiO_2 can introduce energy levels in the band gap, effectively tailoring its electronic structure to absorb light in the visible region. The calculated energy states of N-doped rutile allow us to quantitatively compare the change in the band gap reported by others to the change in the valence band, presuming the conduction band is unaffected by N-doping. In the present study, the N-defect unfilled state was created deeply inside the fundamental conduction band, and this was enough to explain the reason behind the unaffected conduction band of bulk TiO_2. A tailing of the valence band maximum to higher kinetic energy, and an impurity state just above this maximum can be compared to undoped TiO_2. The tail like state was attributed to the N *2p* level, since the binding energy of N *2p* was less than O *2p*, thus extending the valence band maximum to lower binding energy. However, the shift observed in

the valence band of about 0.93 eV, which is enough to explain the observed red shift in optical absorption spectra was reported of about 0.5 - 0.8 eV by several groups. Theoretically, we presented that the N-substitution leads to a tailing of states at the Fermi energy, and this is achieved experimentally. Table 6 displays the produced N-defect state and Fermi energy of the pure rutile. Substitutionally, doped N gave rise to localized N *2p* donor state above the valence band, which was the likely origin of visible light induced photocatalytic activity. The theoretical calculation of energy gap of TiO_2 predicts a reduction by 0.18 - 0.31 eV due to nitrogen atom substitution, in compared to the experimental study, which recorded that the band gap was narrowed by 0.2 eV of N-doped TiO_2. A band gap narrowing is due to the lower binding energy of N *2p* in relation to the O *2p* levels, also a localized dopant N *2p* state is above the O *2p* valence band maximum. Optical absorption measurements of N-doped TiO_2 have shown band gap reduction.

The theoretical investigation of electronic transition states displayed in Figure 9 shows that N-doped rutile exhibits the largest absorption under ultraviolet light irradiation with the value of oscillator strength higher than that of pure rutile, which is in good agreement with UV-visible measurements. Theoretically, we declared a visible absorption for N-doped TiO_2 with strong oscillator strengths, which is in excellent agreement with the experimental spectra of N-doped TiO_2 with absorption at λ>400 nm, which may be interpreted as transference of the electron from the midgap band to CB of N-doped TiO_2.

4. Conclusion

Oxygen vacancy and substitution X-doped rutile (X= B, C and N) have been investigated by Hatree-Fock and density functional theories calculations based on STO-3G basis set. The electronic spectra of these systems are carried out by using PM3 method. The electronic structure and donor states, which may be produced in band gap by oxygen vacancy/ substitution doping, are explored. The oxygen vacancy is a double donor, so the Fermi energy level is moved into the conduction band, thus, there is a significant filling of the defect state. The important electronic transition is induced at the visible range with three peaks which were produced by oxygen point defect. Boron defect produced a half filled electronic state with the same energy of the bottom conduction band. A red shift can be observed in the direct band gap of B-substituted rutile. C-defect produces a filled electron state by 0.5 eV below the fundamental conduction band, and it exhibited significant absorption in the visible region. N-defect unfilled state created deeply inside the fundamental conduction band. N-doped TiO_2 has strong oscillator strengths of absorption at λ>400 nm. The decrease of electron transition energy from the valence band to conduction band may be responsible for the visible light optical absorption in substitution doped TiO_2.

References

Fujishima, A., & Honda, K. (1972), "Electrochemical Photolysis of Water at a Semiconductor Electrode", *Nature* **238**, 37–38.

Nakata, K., & Fujishima, A. (2012), "TiO_2 Photocatalysis: Design and Applications", *Journal of Photochemistry and Photobiology C: Photochemistry Reviews*, **13**, 3, Elsevier, 169-189.

Liu, C., Li, X., & Zu, X. (2009), " Microstructure and Photoluminescence of Carbon and Nitrogen Dual Doped TiO2 Powders", *Chinese J. of Phy.*, **47**, 2, 207-214.

Ali, A. (2012), "Theoretical Investigation for Neon Doping Effect on the Electronic Structure and Optical Properties of Rutile TiO2 for Photocatalytic Applications by Ab Initio Calculations", *Journal of Physical Science*, **23**, 2, 85–90.

Wang, X., Meng, S., Zhang, X., Wang, H., Zhong, W., & Du, Q. (2007) " Multi-Type Carbon Doping Of TiO2 Photocatalyst", *Chemical Physical Letters*, **444,** Elsevier, 292-296.

Cho, E., & Han, S. (2006), " First-principles Study of Point Defects in Rutile TiO_{2-x}", *Physical Rivew B* **73**, American Physical Society, 193202.

Lee, H., Clark, S., & Robertson, J. (2012), " Calculation of Point Defects in Rutile TiO_2 by the Screened-exchange Hybrid Functional ", *Physical Rivew B*, 86, American Physical Society. 075209.

Zhang, J., Wu, Y., Xing, M., Leghari, S., & Sajjad, S. (2010), "Development of Modified N Doped TiO_2 Photocatalyst with Metals, Nonmetals and Metal Oxides," *Energy and Environmental Science*, **3**, 6, 715–726.

Grigorov, K., Oliveira, I., & Maciel, S. (2011), "Optical and Morphological Properties of N-doped TiO_2 Thin Films", *Surface Science*, **605**, 7-8, 775–782.

In, S., Orlov , A., Berg, R., García, F., Pedrosa-Jimenez, S., Tikhov, M., Wright, D., & Lambert, R. (2007) " Effective Visible Light-Activated B-Doped and B,N-Codoped TiO_2 Photocatalysts", *J. Am. Chem. Soc.*, **129** (45),

ACS Publication, 13790–13791.
Jinlong, L., Xinxin, M., Mingren, S., Li, X., & Zhenlun, S. (2010), "Fabrication of Nitrogen-doped Mesoporous TiO_2 Layer with Higher Visible Photocatalytic Activity by Plasma-based Ion Implantation,"
Thin Solid Films, **519**, 1, 101–105.
Janus, M., Choina, J., & Morawski, A. (2009), "Azo Dyes Decomposition on New Nitrogen-modified Anatase TiO2 with High Adsorptivity," *Journal of Hazardous Materials*, **166**, 1, 1–5.
Park, Y., Kim, W., Park, H., Tachikawa, T., Majima, T., & Choi, W. (2009), " Carbon-Doped TiO2 Photocatalyst Synthesized Without Using an External Carbon Precursor and The Visible Light Activity", *Appl. Cataly. B: Enviro.*, **91**, Elsevier, 355-361.
Wang, Y., Feng, C., Zhang, M., Yang, J., Zhang, Z. (2010), "Enhanced Visible Light Photocatalytic Activity of N-doped TiO_2 in Relation to Single-electron-trapped Oxygen Vacancy and Doped nitrogen," *Applied Catalysis B*, **100**, 1-2, 84–90.
Mitoraj, D., Kisch, H. (2008), "The Nature of Nitrogen-modified Titanium Dioxide Photocatalysts Active in vVisible Light," *Angewandte Chemie*, **47**, 51, 9975–9978.
Gorska, P., Zaleska, A., & Hupka, J. (2009), "Photodegradation of Phenol by UV/TiO2 and Vis/N C-TiO_2 Processes: Comparative Mechanistic and Kinetic Studies", *Separation and Purification Technology*, **68**, 1, 90–96.
Hyperchem 7.52, Hypercube Inc., 1115 NW 4th Street, Gainesville, FL 32601, USA (2005).
Shirley, R., & Kraft, M. (2010), " Electronic and Optical Properties of Aluminium-doped Anatase and Rutile TiO_2 from Ab initio Calculations", *Phys. Rev. B*, **81**, American Physical Society 075111.
Pan, G., Jing, W., Qing-Ju, L., & Wen-Fang, Z. (2010), " First-principles Study on Anatase TiO_2 Codoped with Nitrogen and Praseodymium", *Chin. Phys. B*, **19**, 8, 087103.
Di Valentin, D., Finazzi, E., Pacchioni, G. (2007), "N-doped TiO_2: Theory and Experiment", *Chemical Physics*, **339**, 1-3, 44–56.
Cao, F., Tan, K., Lin, M., & Zhang, Q. (2009), "A Density Functional Study of N-Doped TiO_2 Anatase Cluster", *Chinese J. Struct. Chem.*, **28**, 8, 998-1002.
Landmann, M., Rauls, E., & Schmidt, W. (2012)," The Electronic Structure and Optical Response of Rutile, Anatase and Brookite TiO_2", *J. Phys.: Condens. Matter*., **24**, 195503.

Table 1: Dopant elements and their electronic configurations and electronegativities

Atom	Configuration	Elect.
B	1S2 2S2 2P1	2.04
C	1S2 2S2 2P2	2.55
N	1S2 2S2 2P3	3.04

* Oxygen electronigativity is 3.44

Table-2: Conduction band bottom CBb and valence band maximum VBm of rutile and donor states of oxygen vacancy.

	HF	HFVWN	HFPZ81	HFLYP
CBb-TiO_2 (eV)	-2.50	-3.86	-3.86	-3.53
Ov-donor (eV)	-2.61	-4.04	-4.04	-3.67
VBm-TiO_2 (eV)	-4.51	-5.75	-5.75	-5.51

Table 3. Energy difference of the conduction band bottom CB_b of rutile and oxygen vacancy donor level E_v.

	HF	HFVWN	HFPZ81	HFLYP
$CB_b - E_v$ (eV)	0.11	0.18	0.18	0.14

Table 4. Bottom of TiO_2 conduction band and boron defect states, in eV.

	HF	HFVWN	HFPZ81	HFLYP
CB TiO_2	-2.50	-3.86	-3.86	-3.53
B-defect state	-2.63	-3.75	-3.77	-3.53

Table 5. Rutile bottom of CB and upper of VB and induced C-defect states.

	HF	HFVWN	HFPZ81	HFLYP
CB (eV)	-2.50	-3.86	-3.86	-3.53
C-state (eV)	-3.02	-4.22	-4.22	-4.04
VB (eV)	-4.51	-5.75	-5.75	-5.51

Table-6: Rutile Fermi energy and induced N-defect states.

	HF	HFVWN	HFPZ81	HFLYP
E_F (eV)	-3.50	-4.81	-4.81	-4.52
N-state (eV)	-3.58	-4.82	-4.82	-4.56

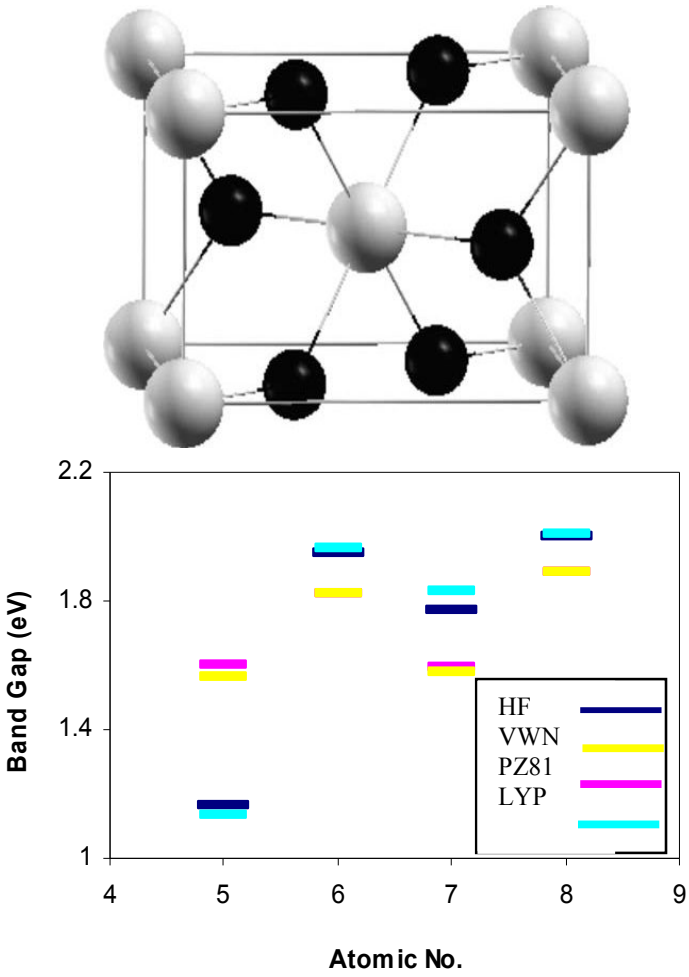

Fig 2: Band gap of rutile vs. atomic number of

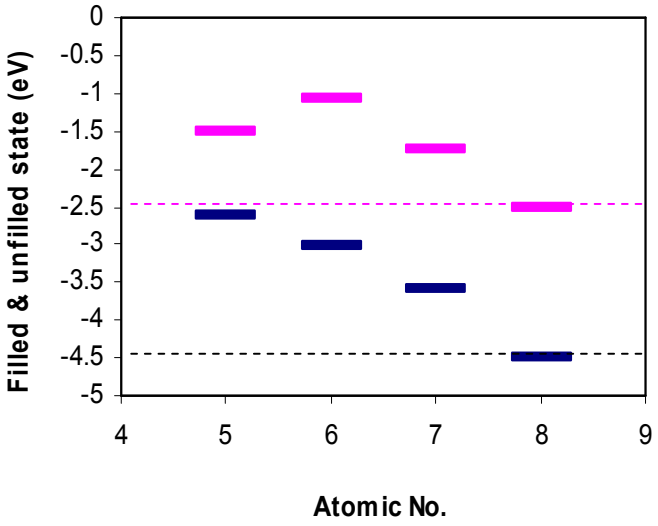

Fig.3: HF cal., filled/unfilled edge of rutile vs. atomic number of dopant.

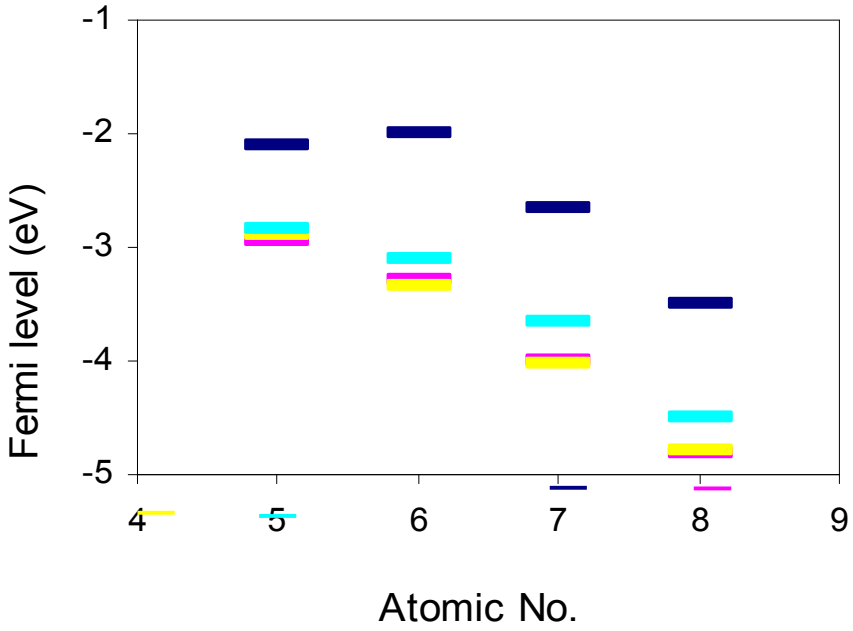

Fig.4: E_F of rutile with/without doping. HF , VWN , PZ81 , LYP .

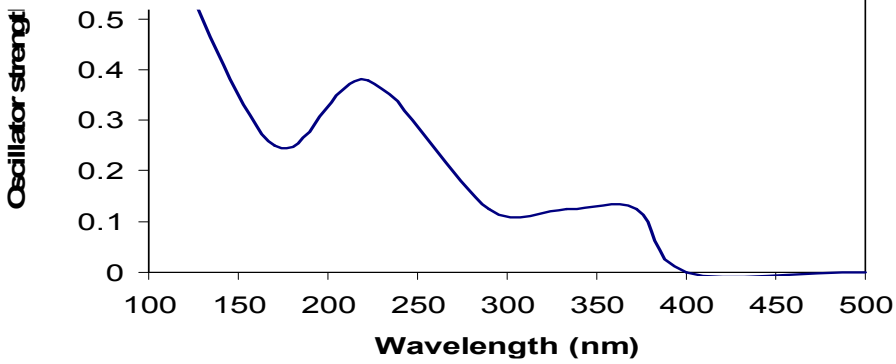

Fig.5: The electronic spectra of rutile.

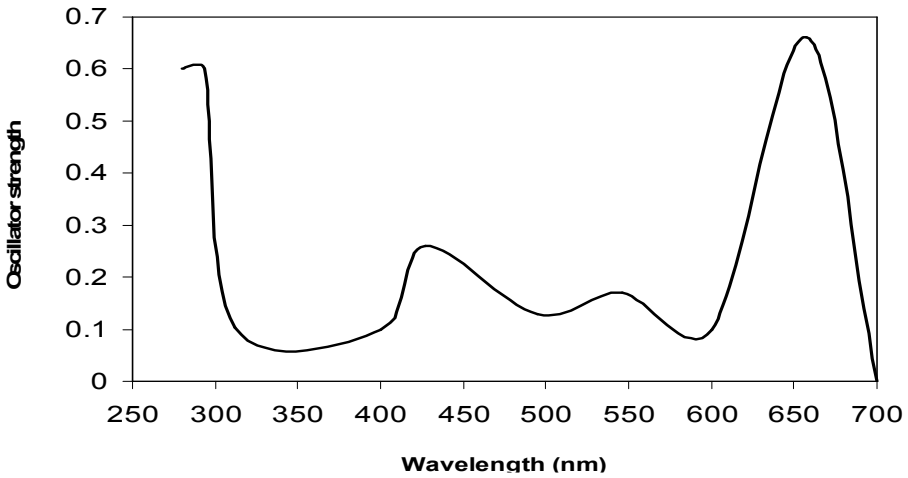

Fig.6: PM3 method, electronic spectra of oxygen vacant rutile.

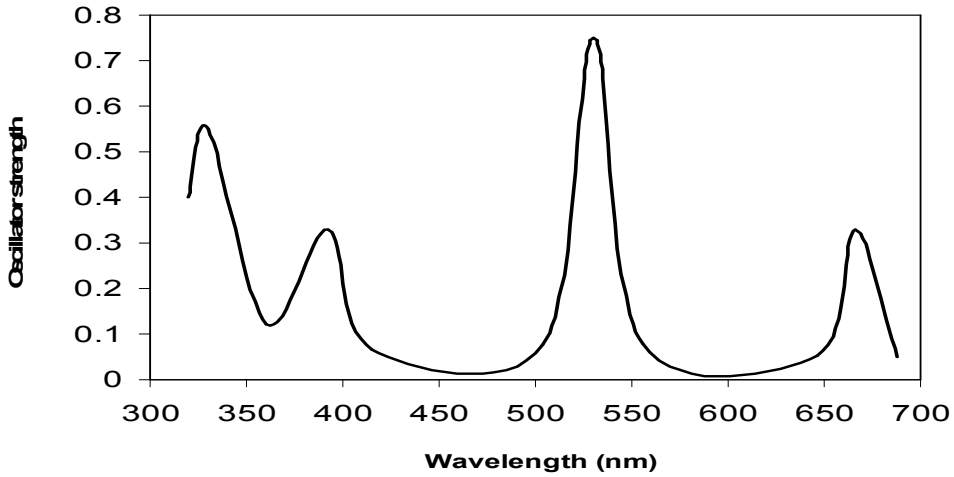

Fig.7: PM3 method, electronic spectra of B-doped rutile.

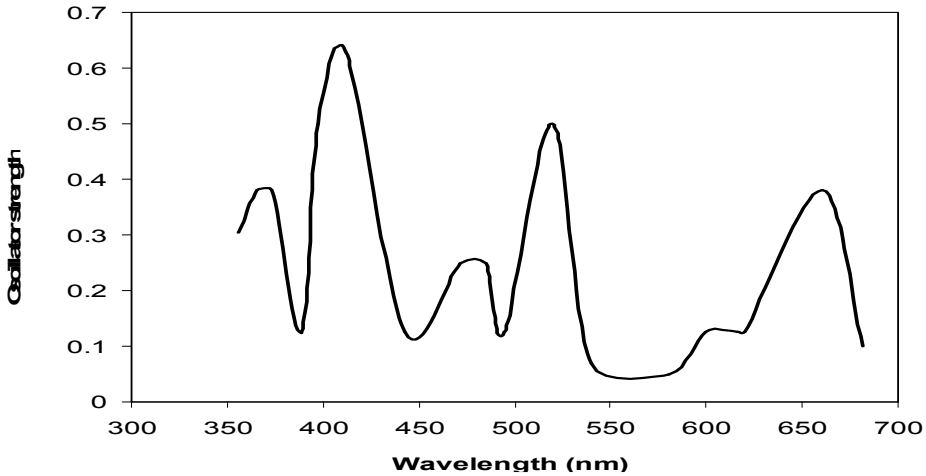

Fig.8: PM3 method, electronic spectra of C-doped rutile.

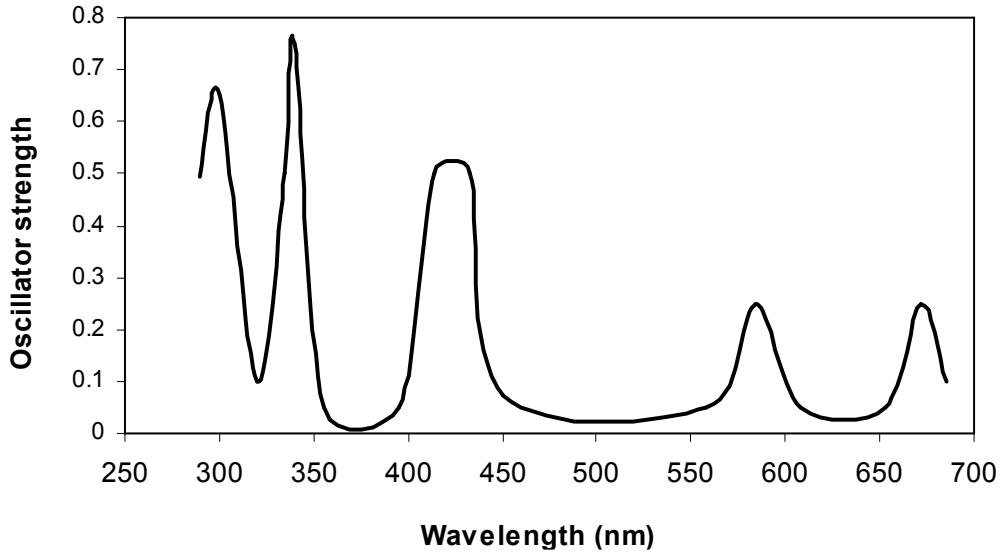

Fig 9:PM3 method, electronic spectra of N-doped rutile.